Journal of Molecular Catalysis A: Chemical 409 (2015) 42–49

Contents lists available at ScienceDirect

Journal of Molecular Catalysis A: Chemical

journal homepage: www.elsevier.com/locate/molcata

Immobilized magnetic nano catalyst for oxidation of alcohol

Pooja B. Bhat[a], Ravindra Rajarao[b], Veena Sahajwalla[b], Badekai Ramachandra Bhat[a,*]

[a] Catalysis and Materials Chemistry Laboratory, Department of Chemistry, National Institute of Technology Karnataka, Surathkal, Srinivasa Nagar 575025, India

[b] Centre for Sustainable Materials Research and Technology (SMaRT@UNSW), School of Materials Science and Engineering, UNSW Australia, Sydney, NSW 2052, Australia

ARTICLE INFO

Article history:
Received 14 April 2015
Received in revised form 20 July 2015
Accepted 12 August 2015
Available online 17 August 2015

Keywords:
Covalent attachment
Schiff base
Magnetic
Oxidation of alcohols

ABSTRACT

Covalent attachment of Schiff base on magnetic nanoparticles yielded good selectivity for oxidation of alcohols. The ferromagnetic interaction in the complex added comprehensive advantage in enhancing the catalytic activity of the nanocatalyst. A greener approach for alcohol oxidation was achieved in solventless method with good yield (>78%). Leaching experiments confirmed a strong interaction between magnetic support and complex. The catalyst showed significant conversion even after 5 catalytic runs.

1. Introduction

Metal(II) complexes coordinating with organic base ligands including Schiff bases are well-known to interact with molecular oxygen to form dioxygen adducts and have extensively been used as efficient and selective homogeneous catalysts for a variety of oxidation reactions in recent years [1,2]. However, the main drawback of these homogeneous catalysts is the necessity of their separation from the reaction mixture at the end of the reaction. Immobilization of Schiff base complexes to the magnetic nanoparticle support *via* covalent attachment provides facile separation of the catalyst during the reaction by external magnet [3]. The magnetic support offers high catalytic efficiency and better recycling without having the inherent problems of leaching of complex/ligand during the reaction.

In recent years, aromatic linkers have been extensively used to immobilize ligands on nanoparticle via click reaction [4,5]. The magnetic superexchange observed in the aromatic linkers such as *m*-phenylene, *p*-phenylene provides stable ferromagnetic interactions between immobilized ligands and the support [6,7]. Recent experimental and theoretical studies on dinuclear metal(II) complexes have shown higher amount of ferromagnetic interaction with bisbidentate bridging ligands bearing *m*-phenylene linkers [8]. Phenelene spacers as linker groups provide aromatic bridging ligand and allow electron exchange between metal and ligand within the framework enhancing magnetic and catalytic activity of the immobilized catalyst.

Schiff base ligand framework forms stable complex depending on the flexibility of the linker group [9]. Schiff base ligands possess the ability to chelate many metal ions and form stable complexes. Researchers have proved that Co(II) and Ni(II) complexes binds with molecular oxygen and the resultant dioxygen–Co and Ni complexes exhibits efficient oxidation reaction [10]. The immobilized supports have shown better control on efficiency of the catalyst due to the microenvironment provided by the support. Hence, immobilized metal complexes have found its advantage in selective oxidation of alcohols with hydrogen peroxide oxidant without any organic solvent, phase transfer catalyst or additive. The redox potential of Co and Ni metal ions influences the decomposition of hydrogen peroxide by reducing its energy of activation and assists in enhancing the catalytic activity of the Schiff bases [11].

Immobilization of Schiff complexes by covalent attachment has proven to be the most effective method for anchoring the metal complexes. Hu et al. have recently reported that Schiff base molybdenum(VI) complexes immobilized onto zirconium poly(styrene-phenylvinylphosphonate)-phosphate showed comparable or even higher conversion and chemical selectivity for epoxidation of olefins compared with other heterogeneous catalysts [12]. The catalysts were easily recovered by simple filtration and were reused with little loss of activity. The potential use of the catalyst for oxidation was reported by Jiang et al. with increased catalytic activity by immobilizing Co salophen complex on montmorillonite [13]. Researchers have explored that higher catalytic activity is observed for oxidation of alcohols to carbonyls

* Corresponding author. Fax: +91 824 2474033.
E-mail address: brchandra@gmail.com (B.R. Bhat).

http://dx.doi.org/10.1016/j.molcata.2015.08.012
1381-1169/

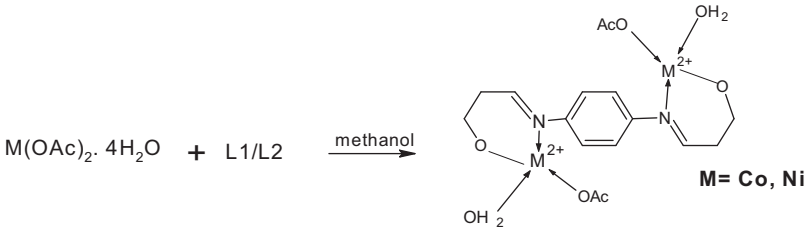

Scheme 1. Schematic representation of complex synthesis.

with efficient separation by immobilized complex on nanoparticle compared to their homogeneous counterparts [14–17].

The primary advantage of immobilization of Co(II) and Ni(II) catalysts is their facile magnetic recovery and the ease with which the reaction products can be separated from the catalysts. The other advantage of this catalyst is the possibility of not requiring solvent and the potential of increased catalytic stability. The geometric structure of the complexes can favour by altering the catalyst activity and selectivity. In recent years, many researchers have devoted on immobilization of the ligands on inert barrier such as silica [18], CNT [19], graphene oxide [20] etc. However, the reported complexes have the drawbacks of excessive loading of complex on magnetic support. Moreover, most of the reported methods are amendable for oxidation reactions by direct condensation of terminal group of the metal complex with chemically modified silane of magnetic support. The superparamagnetic nanoparticles are easily dispersible and have no tendency to aggregate in the solution. Hence, use of superparamagnetic support provides an exceptional behavior for catalytic reactions in solution with easy magnetic recovery. In addition, it would be beneficial if metal complexes are binded with stronger ferromaganetic interactions so as to avoid aggregation of nanocatalyst during catalytic reactions. However, there are very few reports on magnetic interaction between support and immobilized ligands as a stable nanocatalyst for organic reactions. In this work, we have emphasized in studying the possible ferromagnetic interaction to enhance the magnetic and catalytic activity of the nanocatalyst.

2. Experimental

2.1. Materials

Ferrous chloride, ferric chloride, cobalt(II) acetate tetrahydrate and nickel(II) acetate tetrahydrate were purchased from Merck, India and used as received. 3-aminopropyltriethoxysilane was purchased from Sigma–Aldrich and used without further purification.

2.2. Characterization techniques

The FTIR spectra were measured on JASCO FTIR-4200 (KBr technique). 1H NMR was recorded in Bruker instrument using TMS as internal standard. Thermal analysis was carried out (EXSTAR-6000)

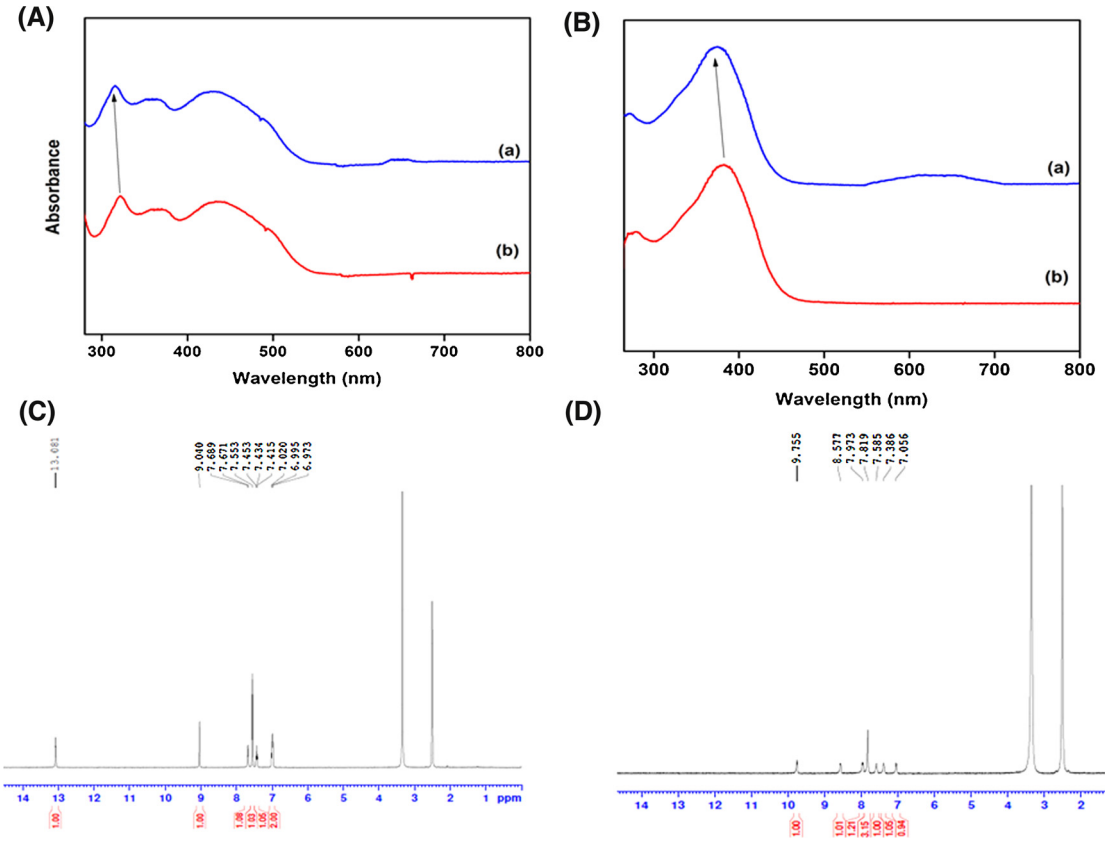

Fig. 1. (A) UV–vis spectrum of (a) complex C1 and (b) ligand L1 (B) UV–vis spectrum of (a) complex C2 and (b) ligand L2 (C) HNMR of L1 and (D) HNMR of L2.

from room temperature to 700 °C at a heating rate of 10 °C/min. The UV–vis spectra were recorded in analytikjena SPECORD S600. Powder X-ray diffraction (XRD) measurements were performed on JEOL JDX 8P diffractometer. The diffraction patterns were recorded at room temperature with Cu Kα radiation (λ = 1.5418 Å) at a scan rate of 2°/min to determine the crystallinity of the sample. Surface morphology and composition was studied by Field emission gun scanning electron Microscopy (FESEM) JSM-7600F and Transmission electron microscope (TEM) Philips CM200. Surface area and pore size distribution was studied by Gemini V2.00 surface analyzer. The magnetic properties were determined by Lakeshore VSM 7410 vibrating sample magnetometer at room temperature.

2.3. Synthesis of ligands and metal complexes

The ligand bis (2-hydroxy benzaldehyde) *p*-phenylenediamine (L1) and bis (2-hydroxy napthaldehyde) *p*-phenylenediamine (L2) was prepared by the drop wise addition of a methanolic solution of *p*-phenylenediamine (1 mmol) to methanolic solution of 2-hydroxy benzaldehyde (2 mmol) or 2-hydroxy napthaldehyde (2 mmol). This resulting solution was refluxed for 2 h. A yellow/red coloured solid mass separated out, which was filtered, washed and subsequently dried. The ligand was found to be insoluble in non polar solvents such as acetone, benzene and soluble in polar solvents like DMF, DMSO. Yield 90% (Scheme 1).

2.4. Synthesis of metal (Ni or Co) complexes

A ligand (L1 or L2) (1 mmol) in the minimum quantity of methanol solution was mixed with a methanolic solution of nickel(II) acetate tetrahydrate or cobalt(II) acetate tetrahydrate (2 mmol). The resulting solution was refluxed with stirring on a magnetic stirrer equipped with heater at 60 °C for 2 h. The bright red (Ni) or dark yellow (Co) colour complex separated out, which was filtered, washed and dried.

2.5. Synthesis of amine functionalized nanoparticle

Magnetic nanoparticles were prepared by chemical coprecipitation technique. Aqueous solution of salts ($Fe_2SO_4{\cdot}7H_2O$) and $FeCl_3{\cdot}6H_2O$ are mixed in D.I. water in 1:2 ratio at 80 °C with slow addition of NH_4OH under anaerobic condition to yield a black ppt. The precipitate was washed with ethanol and water, dried at 80 °C [21,22].

One gram of magnetic nanoparticles was treated with 1.1 g of 3-aminpropyltriethoxysilane (APTES) in presence of toluene at 80 °C for 6 h in argon atmosphere. The product was aged for 1 h and centrifuged with toluene, ethanol and dried at 80 °C (Scheme 2).

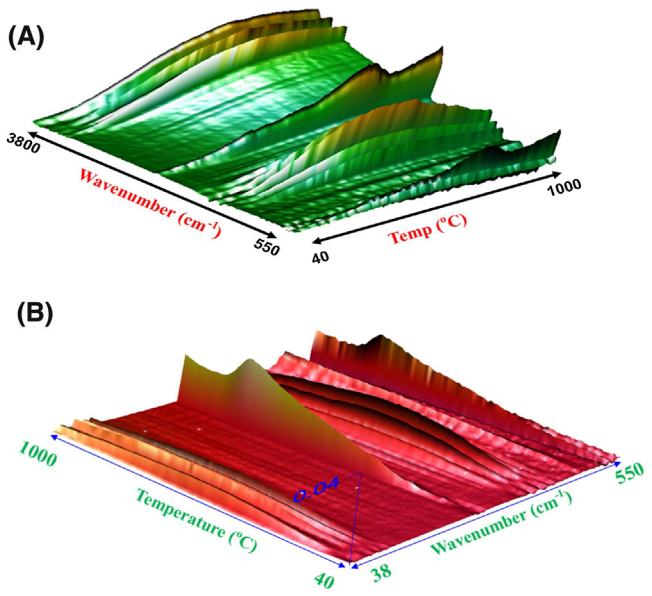

Fig. 2. 3D FTIR of magnetic nanoparticle immobilized (A) Co complex and (B) nickel complex.

2.6. Immobilization of metal complexes on magnetic iron oxide

One gram of amine functionalized ferrite nanoparticles was added to a solution of ligand (C1–C4) complex (100 mg) in 100 mL of dry dichloromethane and the suspension was refluxed for 24 h. After cooling, the brown FCoL1, FCoL2, FNiL1 and FNiL2 nanoparticles were separated using a magnet and were washed several times with dichloromethane and toluene.

3. Results and discussion

The magnetic moments and electronic spectra of ligands and complexes were measured. The magnetic moment values for complexes show that cobalt complexes are paramagnetic in nature and support tetra coordinated configuration. Nickel complexes are diamagnetic in nature. The electronic spectra of the ligand confirmed the presence of intraligand (320 nm and 380 nm) and charge transfer transition at 410 nm respectively (Fig. 1). The ligand L2 showed intraligand transition at 280 nm and charge transfer transition at 390 nm. The complexation was confirmed by the presence of D–D transition at 650 nm. The FTIR spectra of the ligands exhibit a strong band around 1608–1644 cm^{-1}, which is assigned to ν(C=N) vibration. This band is red-shifted in the complexes due to coordination (Figs. 1 and S1). The phenolic band ν(C—O) is observed in the region 1265–1315 cm^{-1} in the free ligand which is shifted to a higher

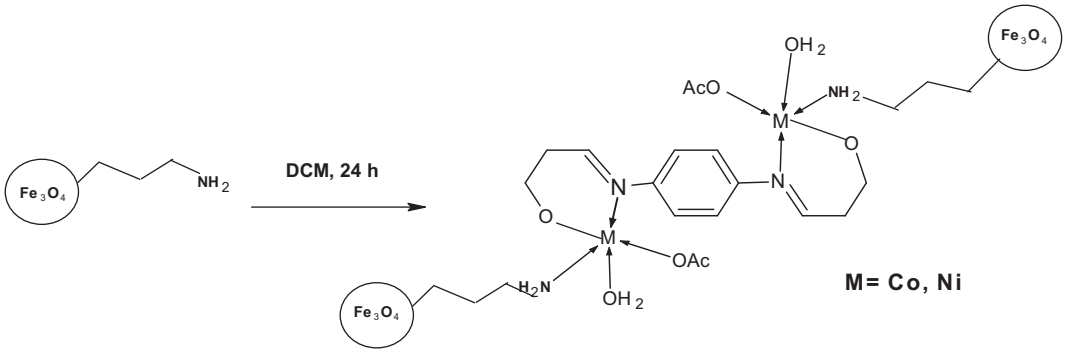

Scheme 2. Schematic representation of MNP-immobilized Schiff base complex.

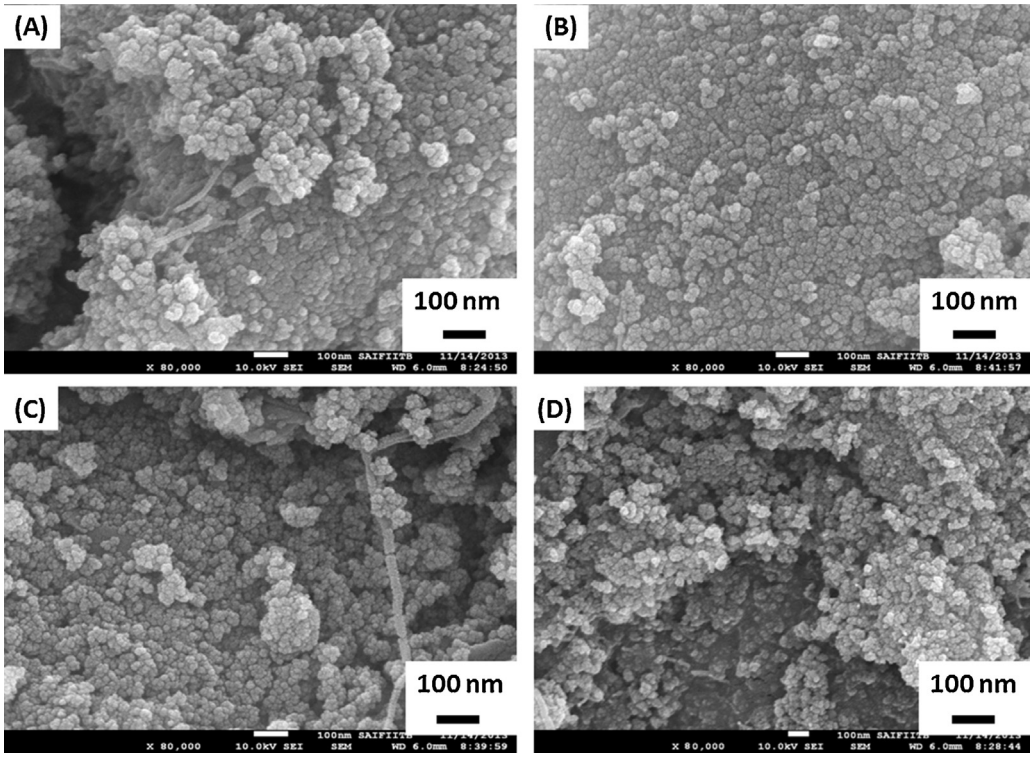

Fig. 3. FEG-SEM of (A) FCoL1, (B) FNiL2, (C) FCoL2 and (D) FNiL1.

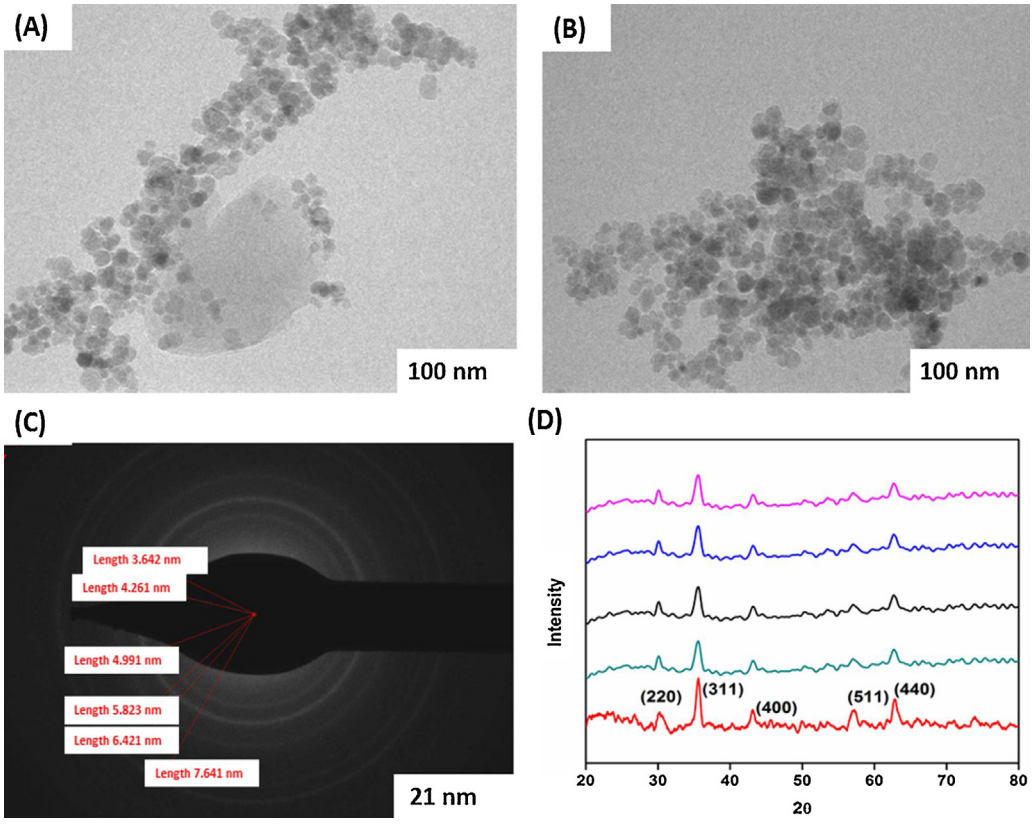

Fig. 4. TEM image of (A) FCoL1 and (B) FNiL1, (C) SAED image, (D) XRD image of (a) Fe_3O_4, (b) FCoL1 (c) FCoL2 (d) FNiL1 and (e) FNiL2.

wave number in the complexes suggesting the coordination of phenolic oxygen to metal ion. Magnetic susceptibility measurements of Co(II) complexes show 4.6–4.7 BM, confirming the tetrahedral structure. HNMR of the ligands confirmed the structure of the ligand (Fig. 1). Due to paramagnetic nature of the Co(II) complex HNMR could not be achieved.

The immobilization of the complex on the magnetic nanoparticle was confirmed by FTIR spectroscopy. The FTIR spectra of grafted complex are similar to that of the free metal complex with Fe—O vibration at 550 cm^{-1}. Physisorbed OH group of ferrite exhibits a broad peak at 3200 cm^{-1} (Figs. 2 and S2). The 3D FTIR spectra further confirms the uniform covalent anchoring of complex on magnetic nanoparticle (Fig. 2). The electronic spectra of the immobilized complexes on magnetic nanoparticle were almost identical to their respective metal complexes indicating that complexes maintain its geometry even after attachment to nanoparticle.

FEG-SEM images of immobilized complexes showed further evidence for the attachment of metal complex to magnetic nanoparticle. It is clearly seen that a bunch of nanoparticle on nanotube like structure is observed (Fig. 3A). TEM images also confirmed the size of nanoparticle to be 40 nm (Fig. 4A). A smoothened surface on nanoparticles (black dots) is observed due to ligand coating. Single Area Electron Diffraction (SAED) shows a bright spherical image (Fig. 4C). This confirms that anchoring metal complexes on the catalyst does not change the crystallinity of the nanocatalyst. X-ray diffraction pattern of immobilized metal complexes was same as raw magnetic nanoparticle, clearly indicates that crystallinity and morphology was not altered after grafting (Fig. 4D). A widened broad spectrum with reduced intensity indicates immobilization of metal complexes on the magnetic nanoparticle.

TG analysis results of FCoL1 and FNiL1 are depicted in Fig. 5. The TG curve recorded under N_2 atmosphere shows a weight loss at temperatures ranging from 35 °C to 800 °C. The decomposition of Schiff base groups is observed in the temperature range from 450 °C to 800 °C. The large weight loss difference between Fe_3O_4-APTES and FCoL1 confirmed anchoring of metal complex on the magnetic nanoparticle. Further, the surface area of the nanocatalyst was studied by BET surface area analysis. Nitrogen sorption isotherms clearly indicated type IV isotherm with mesoporosity (Fig. 6) [23]. Covalent anchored metal complexes on magnetic nanoparticles exhibited surface area of 50 $m^2 g^{-1}$ for FCoL1 and 44 $m^2 g^{-1}$ for FNiL1 respectively. The drastic decrease in surface area of the immobilized complexes compared to bare ferrites is reported. This can be due to blockage of active pores on the surface of nanoparticle by steric ligands.

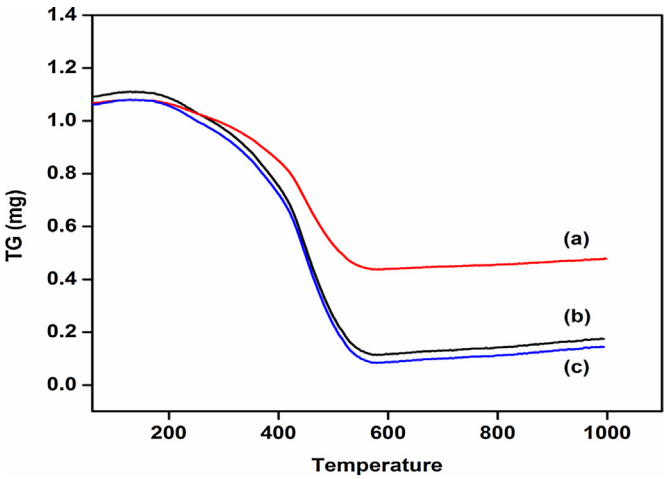

Fig. 5. TG of (a) Fe_3O_4-APTES (b) FCoL1 (c) (b) FNiL1.

The magnetic data was studied by vibrating sample magnetometry. Paramagnetic materials exhibit a linear curve. In this study, a distorted linear curve was obtained which indicated that fer-

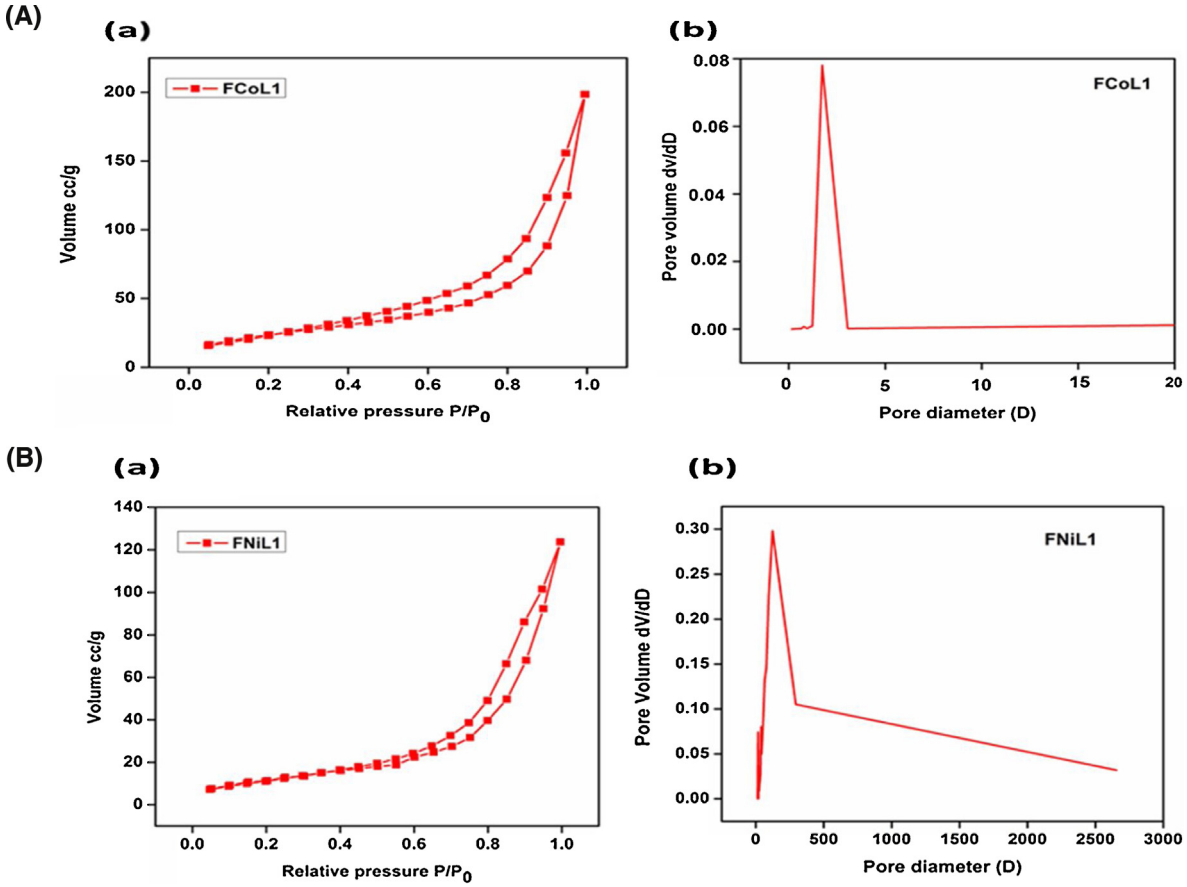

Fig. 6. (a) Nitrogen sorption isotherm and (b) pore size distribution of (A) FCoL1 and (B) FNiL1.

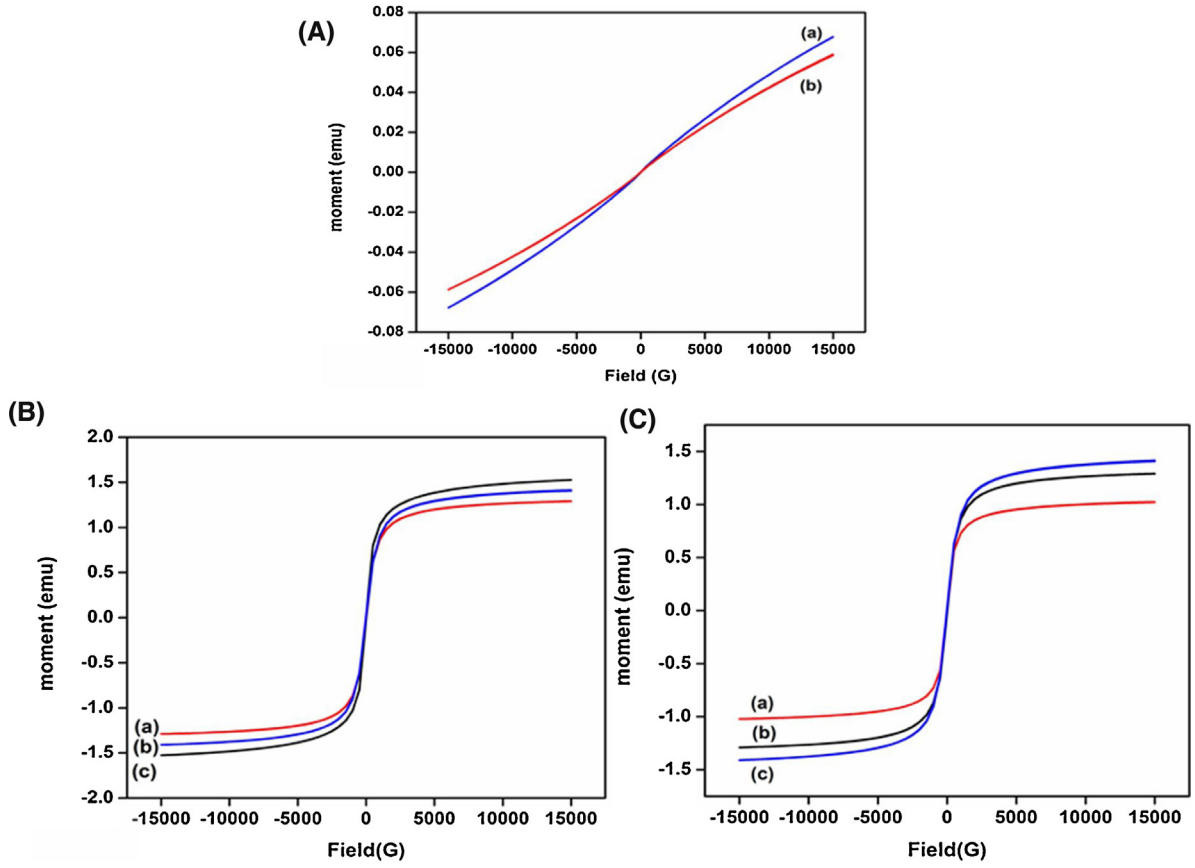

Fig. 7. Vibrating sample magnetometric analysis of (A) complex (a) C1 and (b) C2, (B) magnetic nanoparticles immobilized ligands (a) Fe_3O_4@APTES, (b) FNiL1 and (c) FNiL2, (C) magnetic nanoparticles immobilized ligands (a) Fe_3O_4@APTES, (b) FCoL1 and (c) FCoL2.

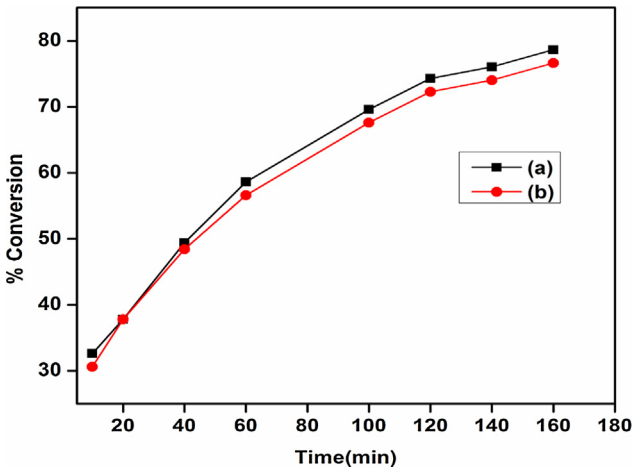

Fig. 8. Effect of time on the catalyst (a) FCoL1 and (b) FNiL1.

Table 1
Optimisation of the catalyst amount and oxidant concentration.

Entry	Catalyst (g)	Amount of oxidant (mmol)	Conversion (%)[a]	
			FCoL1	FNiL1
1	0	5.00	1.6	1.32
2	0.01	5.00	36.0	32.5
3	0.02	5.00	43.5	38.7
4	0.04	5.00	76.6	75.6
5	0.06	5.00	39.7	36.4
6	0.04	0	4.3	4.0
7	0.04	2.00	49.2	42.8

[a] Reaction condition: 1 mmol substrate, time 120 min, temp 80 °C. Average of GC 3 trials.

romagnetic interaction persists in the Co(II) complex. Magnetic curves of Ni(II) complex could not be achieved due to its diamagnetic nature. A hysteresis curve with no coercivity was observed for immobilized complexes on magnetic nanoparticle (Fig. 7B). Higher amount of saturation magnetization is observed due to ferromagnetic interaction in the Co(II) complex. This is confirmed by increase in saturation magnetization of the immobilized Co(II) complex compared to bare magnetic nanoparticle.

The oxidation of alcohols to carbonyls was studied in detail by optimizing the reaction variables such as solvent, alcohol/oxidant, alcohol/catalyst molar ratio and length of reaction time. Benzyl alcohol was used as model substrate and the reaction product analysis was carried out using Gas Chromatography (GC) (Shimadzu 2014, Japan); the instrument has a 5% diphenyl and 95% siloxane Restek capillary column (30 m length and 0.25 mm diameter) and Flame Ionization Detector (FID). The initial column temperature was increased from 60 °C to 150 °C at the rate of 10 °C/min and then to 220 °C at the rate of 40 °C/min. Nitrogen gas was used as the carrier gas. The temperature of the injection port was kept constant at 150 °C and 250 °C respectively during product analysis. The retention time for different compounds was determined by injecting pure compounds under identical GC conditions.

All reactions were carried out in a glass reactor (~50 mL) with benzyl alcohol (1 mmol) as model substrate. The optimized amount of nano catalyst (0.04 g), H_2O_2 (30 wt% in water) was added to the reaction mixture and vigorously stirred at optimized reaction conditions. The aliquots of the reaction mixture were analysed by GC. The GC conversion with acetonitrile as a solvent did not show a significant change in catalytic activity when compared

with solventless method. This confirmed that solvent does not play any role during catalysis. Further, higher rate of conversion was observed for solventless method at temperature of 80 °C. The effect of time on the activity was studied at regular intervals of time under similar reaction conditions (Fig. 8). The maximum conversion was observed at the end of 120 min for the immobilized metal complexes. The reaction was optimized for different catalyst to substrate ratios. The oxidation of alcohols wasn't initiated in the absence of catalyst (Table 1, entry 1 and 6). A 0.04 g of catalyst was sufficient for the effective transformation of (1 mmol) benzyl alcohol to benzaldehyde with hydrogen peroxide (5 mmol) as terminal oxidant.

The anchoring of complex on ferrite (Fe_3O_4) could result in a favourable combination of heterogeneous and homogeneous catalysis. Additionally, the magnetic support can provide a stabilizing effect and can assist in easy recovery of the catalyst during due course of the reaction. The influences of the immobilized metal complexes in catalysis were investigated on the model substrate in identical reaction conditions and are summarized in Table 2. Bare ferrite showed very less conversions <16.6%. The catalytic activity was slightly higher for covalently immobilized metal complexes than their homogeneous counterparts. The magnetic support suppresses the formation of bridged complexes and prevents the catalyst deactivation.

The oxidation was further extended to a variety of alcohols including aromatic and aliphatic alcohols (Table 3). All the alcohols studied were oxidized smoothly to give aldehydes with complete selectivity for aldehydes. All the experiments were carried out in air atmosphere at temperature of 80 °C. This indicated that oxidation involves peroxide adsorption on the surface of nanoparticles followed with decomposition of peroxide at high temperature to assist oxidation. Higher catalytic activity was observed for immobi-

Table 2
Comparison of immobilized metal complex nanocatalyst with bare ferrite and complexes.

Entry	Catalyst	Conversion (%)[a]	Selectivity	TOF_{obs} (h^{-1})[b]
1	Nano Fe_3O_4	16.6	>99	–
2	CoL1	68.2	>99	–
3	CoL2	72.6	>99	–
4	NiL1	65.8	>99	–
5	NiL2	67.3	>99	–
6	FCoL1	76.6	>98	36.1
7	FCoL2	78.0	>98	41.0
8	FNiL1	75.3	>98	38.5
9	FNiL2	74.2	>98	41.1

[a] Reaction conditions: substrate (1 mmol); oxidant (H_2O_2, 30%, 5 mmol); catalyst (0.04 g); time 120 min. Conversion and selectivity are determined by GC. Average of GC 3 trials.

[b] TOF values were calculated by [(malcohol × X/mcatalyst)/D] × *t*, X = Conversion of benzyl alcohol as determined by GC, D = wt% of Ni in the catalyst, *t* = reaction time.

Table 3
Oxidation of alcohols catalyzed by MNP immobilized Schiff base metal complexes.

Substrate	Product	% Yield of carbonyl compound[b]			
		FCoL1	FCoL2	FNiL1	FNiL2
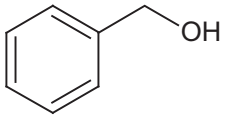	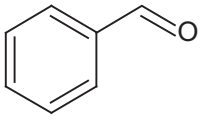	76.6	78.0	75.3	74.2
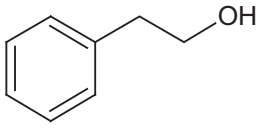	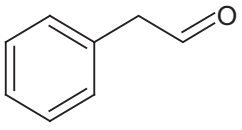	96.5	94.3	92.6	90.0
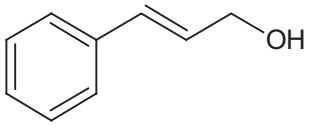	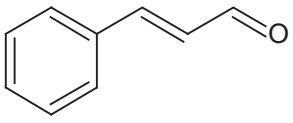	95.8	94.3	90.30	93.3
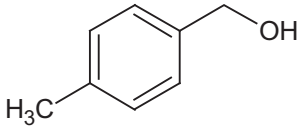	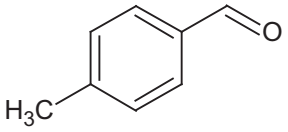	68.3	66.8	69.5	65.2
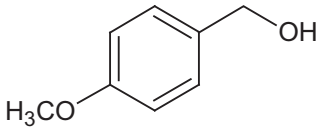	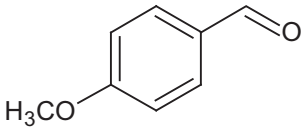	65.4	66.7	62.5	63.1
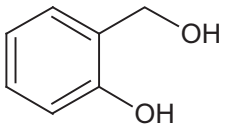	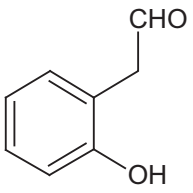	64.0	61.9	60.4	58.0

Table 3 (*Continued*)

Substrate	Product	% Yield of carbonyl compound[b]			
		FCoL1	FCoL2	FNiL1	FNiL2
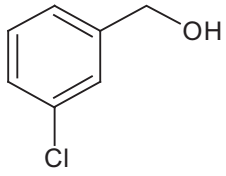	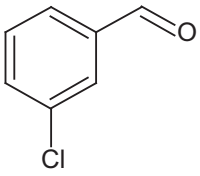	68.7	70.3	66.6	68.9
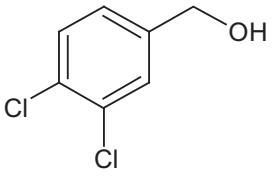	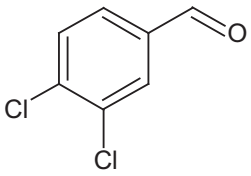	72.3	70.5	70.4	69.4
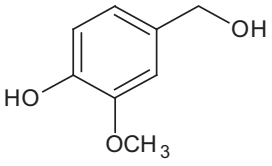	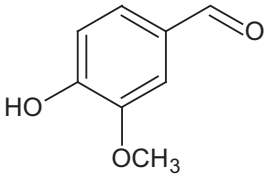	73.2	70.6	66.9	71.5
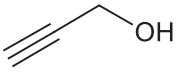	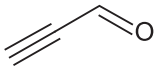	32.6	32.3	29.7	30.9
$(CH_3)_2CH_2OH$	$(CH_3)_2CHO$	27.2	24.3	21.4	25.9

[a] Reaction conditions: substrate (1 mmol); oxidant (H_2O_2, 30%, 5 mmol); catalyst (0.04 g); time 120 min, temp 80 °C, solventless.
[b] Average of 3 GC trials.

lized Co(II) complex compared to immobilized Ni(II) complex. The magnetic nanocatalyst was recycled efficiently by simple magnetic extraction and exhibited good conversion even after 5 catalytic runs (Fig. 4 and S4) Leaching experiments confirmed that the nanocatalyst is truly heterogeneous and that no catalytically active Ni or Co species are dissolved in the solution (Table S1). Negligible amount of leaching during oxidation process confirms a strong interaction between magnetic support and metal complexes.

4. Conclusions

We have successfully synthesized magnetic nanoparticle immobilized metal complexes. A promising greener approach with high catalytic activity for oxidation of primary and secondary alcohols was achieved. Ferromagnetic interaction in the Co(II) complex enhanced the catalytic activity of the immobilized complex. The immobilized metal Schiff base complexes were catalytically active in solventless system and yielded efficient anchoring. The advantages of immobilized metal complex catalyst are high catalytic, stability and facile reusability.

Acknowledgement

The author Pooja would like to thanks NITK for research fellowship, CRNTS-Bombay for FEGSEM and TEM facility, NITK metallurgy department for research assistance. The author would also like to thank Dr. Ravindra for research assistance.

Appendix A. Supplementary data

Supplementary data associated with this article can be found, in the online version, at http://dx.doi.org/10.1016/j.molcata.2015.08.012.

References

[1] S. Velusamy, A. Srinivasan, T. Punniyamurthy, Tetrahedron Lett. 47 (2006) 923–926.
[2] K. Kervinen, H. Korpi, M. Leskela, T. Repo, J. Mol. Cat A: Gen. 203 (2003) 9–19.
[3] M. Kooti, M. Afshari, Catal. Lett. 142 (2012) 319–325.
[4] B.S. Rana, S.L. Jain, B. Singh, A. Bhaumik, B. Sain, A.K. Sinha, Dalton Trans. 39 (2010) 7760–7767.
[5] H. He, Y. Zhang, C. Gao, J. Wu, Chem. Commun. (2009) 1655–1657.
[6] C. Yuste, J. Ferrando-Soria, D. Cangussu, O. Fabelo, C. Ruiz-Perez, N. Marino, G.D. Munno, S.E. Stiriba, R. Ruiz-Garcia, J. Cano, F. Lloret, M. Julve, Inorg. Chim. Acta 363 (2010) 1984–1994.
[7] A. Nabei, T. Kuroda-Sowa, T. Shimizu, T. Okubo, M. Maekawa, M. Munakata, Polyhedron 28 (2009) 1734–1739.
[8] M.A. Palacios, A. Rodriguez-Dieguez, A. sironi, J.M. Herrera, A.J. Moto, J. Cano, E. Colacio, Dalton Trans. (2009) 8538–8547.
[9] P.G. Cozzi, Chem. Soc. Rev. 33 (2004) 410–421.
[10] S. Jain, O. Reiser, ChemSusChem 1 (2008) 534–541.
[11] K.C. Gupta, A.K. Sutar, J. Macromol. Sci. Part A: Pure Appl. Chem. 44 (2007) 1171–1185.
[12] Z. Hu, X. Fu, Y. Li, Inorg. Chem. Commn. 3 (2011) 497–501.
[13] J. Jiang, K. Ma, Y. Zheng, S. Cai, R. Li, J. Ma, Appl. Clay Sci. 3 (2009) 117–122.
[14] S. Jain, O. Reise, ChemSusChem 1 (2008) 534–541.
[15] S.P. Shylesh, J. Schweizer, S. Demeshko, V. Schünemann, S. Ernst, W.R. Thiel, Adv. Synth. Catal. 351 (2009) 1789–1792.
[16] M. Mohammadikish, M. Masteri-Farahani, S. Mahdavi, J. Magn. Magn. Mater. 354 (2014) 317–323.
[17] M. Bagherzadeh, M.M. Haghdoost, F.M. Moghaddam, B.K. Foroushani, S. Saryazdi, E. Payab, J. Coord. Chem. 66 (2013) 3025–3036.
[18] L. Tian, X. Lou, Z.Q. Pan, Q.M. Huang, H. Zhou, Micro Nano Lett. 8 (2013) 159–162.
[19] R. Rajarao, T.H. Kim, B.R. Bhat, J. Coord. Chem. 65 (2012) 2671–2682.
[20] Z. Li, s. wu, H. Ding, D. Zheng, J. hu, X. Wang, Q. Huo, J. guan, Q. Kan, New. J. Chem. 37 (2013) 1561–1568.
[21] R. Valenzuela, M.C. Fuentes, C. Parra, J. Baeza, N. Duran, S.K. Sharma, M. Knobel, J. Freer, J. Alloys Compd. 488 (2009) 227–231.
[22] P.B. Bhat, B.R. Bhat, New J. Chem. 35 (2015) 273–278.
[23] K.S.W. Singh, Pure Appl. Chem. 57 (1985) 603–619.